JOURNAL OF PROPULSION AND POWER
Vol. 25, No. 1, January–February 2009

Cryogenic Flow and Atomization from a Coaxial Injector

V. Gautam* and A. K. Gupta†
University of Maryland, College Park, Maryland 20742

DOI: 10.2514/1.28921

The global flow characteristics of the cryogenic flow injected from a single-element coaxial injector have been examined experimentally to simulate the flow and mixing behavior before ignition and combustion in characteristic rocket engines. The injector simulated one element of the cryogenic rocket engine injectors under realistic operating conditions. This work focuses specifically on the evolution of liquid nitrogen jet instability, spreading, and its atomization and mixing with the surrounding coaxial gaseous jet under steady-state atmospheric conditions. The effect of some important flow parameters, such as velocity ratio and momentum ratio between jets, on the potential core length of the liquid nitrogen jet and shear angle of the flow have been analyzed. The results showed a significant role of these parameters on the instability and breakup of the liquid nitrogen jet, along with the strong heat transfer effect of the surrounding atmosphere on the cryogenic liquid nitrogen jet. The shear angle of the flow remained constant along the longitudinal axis of the injector, thus confirming fully developed steady-state jet under atmospheric conditions. The mean value of the shear angle showed the transcritical nature of the liquid nitrogen jet under atmospheric conditions. The shear angle of the flow also reduced with introduction of the helium jet and decreased uniformly with increase in helium jet velocity, which supports the effect of surrounding gas density on the jet spreading as predicted by previous researchers. The potential core length of the cryogenic liquid nitrogen showed a local peak as a function of velocity of the gaseous jet and decreased exponentially with momentum ratio for values close to and higher than one.

I. Introduction

ANALYZING the cryogenic flow from a coaxial injector is one of the most crucial areas of interest associated with state-of-the-art rocket engine technology. Significant research has been conducted in this area to study the behavior of coaxial jets using single-phase gaseous jets and two-phase jets using water or some other subcritical fluid [1–4]. Single-phase coaxial jets are, in general, very well understood because of their extensive investigation by various researchers, for not only rocket engine applications but also in other combustion systems. However, the destabilization, disintegration, and mixing of cryogenic jets in the presence of a high-speed coaxial surrounding gaseous jet are still relatively less understood phenomena, in spite of numerous past attempts to study them. Thus, the objective of this research is to analyze some of the key flow parameters, such as liquid core length and flow shear angles, for coaxial jets using cryogenic fluid.

In case of cryogenic fluids, analyzing the flow behavior of the jet, its destabilization, disintegration, and evaporation becomes complicated, because of huge variations in physical properties and nonisothermal flow conditions. The destabilization of a liquid jet in a two-phase coaxial flow takes place due to several complex physical processes, such as the development of a shear layer due to velocity gradients, the turbulent interactions and vorticity produced by the boundary layer, and the interaction between inertial, surface tension and viscous forces. A combination of all of these destabilization processes, along with the complex thermophysical processes related to phase change, makes it very challenging to understand and analyze the flow and atomization behaviors of two-phase cryogenic flows [5–7].

Previous research has also identified some important parameters that affect the physical processes, such as physical and chemical properties of the fluids, velocity and density ratios between the jets, inlet temperature of the fluids, shape and geometry of the injector exit, recess length of the injector, presence of swirl to the flow, and temperature and pressure of the mixing chamber. Reitz and Bracco [8] performed extensive experiments with water jets and showed that the growth rate or spray angle of an isothermal jet depends strongly on the densities of the liquid jet and surrounding gas, that is, $\theta \approx 0.27(\rho_g/\rho_l)^{0.5}$. Chehroudi et al. [9,10] investigated cryogenic jets (LOX and LN_2) initially at a subcritical temperature injected into supercritical temperature environment and at various pressures ranging from subcritical to supercritical values. They finally improved Reitz and Bracco's model [8] to predict the growth rate of a shear layer by using their experiments, given as $\theta = 0.27\{F[x(\rho_g/\rho_l)] + (\rho_g/\rho_l)^{0.5}\}$.

Gautam and Gupta [11], Strakey et al. [12], and Villermaux [13] have shown that the momentum flux ratio ($M = \rho_g v_g^2/\rho_l v_l^2$) is one of the key parameters for single-phase or two-phase coaxial jet mixing. They demonstrated that the lengths of the potential cores, and the liquid-jet breakup and mixing with the surrounding gases, are significantly affected by the momentum flux ratio between the jets. In their earlier works, Villermaux and Rehab [14], Farago and Chigier [15], Rehab et al. [16], and Lasheras et al. [17] provided some characterization of coaxial jets using noncryogenic fluids. Lasheras and Hopfinger [4] also provided an improved correlation for prediction of potential core lengths, as shown by Eq. (1):

$$L_b/D_l = 6M^{-0.5}(1 - 0.001\sigma/\mu_g V_g)^{-0.5} \tag{1}$$

Although some of the aforementioned investigators did not examine the relevant rocket injector conditions, the results obtained from these investigations provided important insightful information and means for extrapolating the results to the characteristic rocket injector operational conditions. Some other more relevant work has been reported on the behavior of cryogenic fluids under high-pressure subcritical and supercritical conditions. Pal et al. [18], Vingert et al. [19] and Mayer et al. [20–23] studied the high-pressure injection and mixing processes of cryogenic propellants under nonreacting conditions using LN_2 as a simulant for LOX. Porcheron et al. [24] investigated the core length of an LOX jet in a coaxial gaseous stream (He, N_2, and Ar). They performed experiments for a large range of momentum ratios ($M \sim 2$–21.6) by varying the velocities and densities of the jets and proposed a correlation [Eq. (2)]

Received 7 December 2006; revision received 10 March 2008; accepted for publication 4 May 2008. Copyright © 2008 by the authors. Published by the American Institute of Aeronautics and Astronautics, Inc., with permission. Copies of this paper may be made for personal or internal use, on condition that the copier pay the $10.00 per-copy fee to the Copyright Clearance Center, Inc., 222 Rosewood Drive, Danvers, MA 01923; include the code 0748-4658/09 $10.00 in correspondence with the CCC.

*Graduate Student, Mechanical Engineering Department. Student Member AIAA.

†Distinguished University Professor, Mechanical Engineering Department; akgupta@eng.umd.edu. Fellow AIAA.

to predict the potential core length of the LOX jet based on momentum ratio, Ohnesorge number Oh, and density ratio between the jets:

$$L_b/D_l \approx 2.85(\rho_g/\rho_l)^{-0.38} Oh^{0.34} M^{-0.13} \quad (2)$$

In another, more recent, study, Oschwald et al. [25] investigated the effect of chamber pressure, initial jet temperature, and acoustic waves on the atomization, mixing, and combustion phenomena of LOX/H_2 coaxial rocket injectors. Gautam and Gupta [26–28] studied the flow and evaporation characteristics of cryogenic fluids under normal atmospheric conditions to gain insight on the initial mixing that affects the ignition. Davis and Chehroudi [29] developed an automated method for measurement of the dark-core lengths (potential core lengths) from a large number of flow images and showed that the dark-core length decreases at higher chamber pressures, due to the combined effects of inner tube heat transfer and better interjet mixing. The length of the dark core shortened with increase in velocity ratio at constant chamber pressure, and asymptotically approached a constant value. Their results also showed the dependence of the gas/liquid momentum ratio to an exponent, with the exponent having a different value for subcritical pressures as opposed to near- and supercritical pressures. However, in spite of all these research efforts, attaining comprehensive understanding of the liquid breakup, dispersion, evaporation, and mixing of cryogenic fluids under all relevant and realistic operating conditions is still a major challenge involving highly complicated phenomena.

This study analyzes the physical characteristics of a cryogenic LN_2 jet surrounded by a coaxial gaseous stream at normal atmospheric pressure conditions, using a high-speed schlieren diagnostic technique. Specifically, the characteristic inner potential core lengths and shear angles have been examined for different velocities of the surrounding gaseous jet. The experimental matrix allowed for detailed examination of some of the important flow parameters, such as the velocity and momentum ratios between the jets.

II. Experimental Setup and Condition

The experimental facility consisted of a supply system for cryogenic liquid nitrogen and gaseous helium, a single-element coaxial injector, and an exhaust system. A schematic diagram of the injector tubes, along with the injector face plate, with dimensions through which the flows emerge is shown in Fig. 1. The inner injector tube has inner diameter of $D_l = 0.33$ in. (8.4 mm) with a wall thickness of 0.02 in. (0.5 mm). The dimensions of the injector have been chosen after consultation with industrial manufacturers, and the injection areas of the two flows have been kept constant, which is generally the case for shear coaxial rocket injectors. The flows of the gaseous and cryogenic fluids into the experimental facility were controlled using fast response (<50 ms) solenoid valves to obtain temporal resolution on the evolutionary behavior of the flow upon exit from the injector.

The flow rate of the gaseous jet was measured using precision orifices preceded with a digital pressure sensor. The average temperature of the gaseous flow at the injector exit was measured using a thermocouple and was found to be 263 K, and the velocity was calculated under the assumption of ideal gas density. The flow rate of LN_2 was measured using a liquid turbine flowmeter. However, to assure that the measurement values were accurate, the flowmeter had to be cooled to LN_2 temperature before getting steady-state accurate readings. This procedure ensured liquid flow through the flowmeter with minimum vapor formation. Note that any vapor formation will result in erroneous readings from the turbine flowmeter. Therefore, the procedure of acquiring LN_2 flow rate measurements starts by bleeding LN_2 at very low flow rates, until the temperature of flowmeter reaches the LN_2 cryogenic temperature. A thermocouple was used to monitor online the temperature immediately upstream of the turbine flowmeter. Once this was achieved, the LN_2 valve was opened completely to allow the flow to stabilize for few seconds before starting the measurements. This approach assured that the variations in flow rate were reduced to less than 5%. The flow rate through the injector was also calculated using Bernoulli's equation by measuring pressures upstream and downstream of the coaxial injector. The difference in measured flow velocity from the pressures across the injector and turbine flow meter readings was less than ±5% for several different test runs, which is actually quite reasonable for a cryogenic fluid that posseses complex flow and heat transfer characteristics. The volumetric flow rate of LN_2 was fixed at 4.5 gal/min (0.23 kg/s) for all experiments conducted in this study, with an average temperature and density of the LN_2 jet at the injector exit taken as 77 K and 808 kg/m^3, respectively.

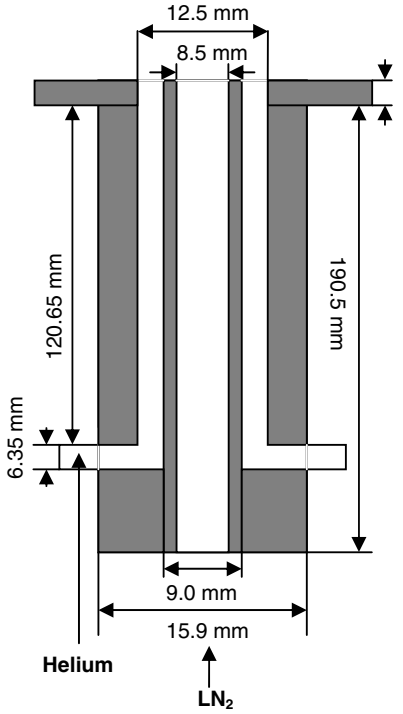

Fig. 1 Schematic diagram of the coaxial injector setup with dimensions.

The experimental test matrix of the flow conditions examined in this paper is given in Table 1. Experiments were performed to analyze the effect of gas velocity and momentum ratio on the flow characteristics of the cryogenic jet. For the experiments, the velocity of the liquid nitrogen jet was kept constant at 5 m/s, whereas the velocity of the helium jet was varied from no flow to 630 m/s. The typical velocity and momentum ratios for practical rocket injectors are approximately in the range of 20–30 and 5–10, respectively. The Reynolds and Weber numbers of the LN_2 jet calculated at 77 K and 1 atm were found to be 2.21E + 05 and 1.93E + 04, respectively.

III. Data Acquisitions and Analysis

Schlieren clips of the full flowfield have been obtained using a high-speed camera framing rate of 512 frames/s at a resolution of 1024 × 512 pixels. The camera responds to visible wavelengths of the spectrum. Data analysis for the present set of experiments included obtaining time-resolved images from the high-speed movies and applying image processing techniques on those images to calculate the averaged potential core lengths and shear angles for the various test cases. The MATLAB image processing toolbox is used for all the data analysis.

Figure 2a shows an instantaneous high-speed schlieren image of a steady-state LN_2 jet in a coaxial He flow. This image shows the development of the shear layer between the two flows. Initially, a stable liquid jet (dark region) can be seen emerging from the injector exit along with the coaxial He stream (light region) until around 2 diameters downstream. This is an indication of initial mixing zone where the two jets have little or no interaction with each other. As the

Table 1 Test matrix for the flow inlet conditions examined

Case no.	Inner fluid	Outer fluid	Velocity, m/s, liquid/gas	Density ratio, gas/liquid	Momentum ratio, gas/liquid	Mass ratio, gas/liquid
1	LN_2	He	5/0	——	0	——
2	LN_2	He	5/5	2.3E − 04	2.3E − 04	2.4E − 04
3	LN_2	He	5/10	2.3E − 04	9.2E − 04	4.8E − 04
4	LN_2	He	5/20	2.3E − 04	3.7E − 03	9.7E − 04
5	LN_2	He	5/30	2.3E − 04	8.3E − 03	1.5E − 03
6	LN_2	He	5/40	2.3E − 04	14.7E − 03	1.9E − 03
7	LN_2	He	5/50	2.3E − 04	23.0E − 03	2.4E − 03
8	LN_2	He	5/100	2.3E − 04	91.9E − 03	4.9E − 03
9	LN_2	He	5/150	2.3E − 04	0.21	7.2E − 03
10	LN_2	He	5/200	2.3E − 04	0.37	9.7E − 03
11	LN_2	He	5/250	2.3E − 04	0.57	1.2E − 02
12	LN_2	He	5/300	2.3E − 04	0.83	1.4E − 02
13	LN_2	He	5/325	2.3E − 04	0.98	1.6E − 02
14	LN_2	He	5/350	2.3E − 04	1.13	1.7E − 02
15	LN_2	He	5/390	2.3E − 04	1.4	1.9E − 02
16	LN_2	He	5/460	2.3E − 04	1.95	2.2E − 02
17	LN_2	He	5/500	2.3E − 04	2.3	2.4E − 02
18	LN_2	He	5/565	2.3E − 04	2.92	2.7E − 02
19	LN_2	He	5/630	2.3E − 04	3.68	3.0E − 02

flow progresses further downstream, the formation of vortical structures, as a result of shear-layer development, destabilized the inner liquid core to break up and mix with the surrounding gases. The cryogenic jet expansion θ and potential core length L_b associated with the unstable LN_2 jet can also be observed from Fig. 2a. Figure 2b shows an average of 150 high-speed schlieren images for the same case. This image was obtained to enable the calculation of the average shear angles and potential core lengths. It can be seen that the vortical structures are not visible for the averaged case anymore, because of the cancellation and smoothening of the flow structures during the averaging process. In both parts of Fig. 2, however, the LN_2 jet is opaque to the light and thus appears dark (because of the very low light intensity, close to zero, in this region), whereas the surrounding gases are brighter and have a higher light intensity (close to 240).

Figure 3 shows the variation of light intensity with radial distance at various axial locations, obtained from the averaged schlieren image. This plot was obtained to show the liquid-jet expansion and calculation of shear angle between the jets. One can see the presence of a symmetric, highly dense, dark liquid core (intensity close to zero) along with its expansion over the axial distance, as it progresses further downstream from the injector exit. The jet width w of the flow is defined as the distance between the two points where the radial intensity reached half of the maximum intensity, that is, 120. These two points, and consequently the width of the flow, were determined after processing the image using image processing techniques. The shear angle (Fig. 4) of the flow was calculated at different axial distances y based on the jet width according to Eqs. (3) and (4):

$$\tan(\theta/2) = 0.5 \text{ jet width/equivalent axial distance} \tag{3}$$

$$\therefore \tan(\theta/2) = 0.5(w - D_l)/y \tag{4}$$

Figure 5a shows axial distribution of the averaged centerline intensity obtained from the averaged image. The centerline intensity was plotted to show the behavior of the LN_2 jet quantitatively, as it progresses downstream of the injector exit. The increase in centerline intensity indicates the decrease in density of the fluid at the centerline to reveal the process of LN_2 jet breakup and mixing with the surrounding gases. The increase in centerline intensity (decrease in fluid density) remains low and insignificant, until the breakup length of the liquid potential core is reached. Beyond this point, the liquid jet breaks into droplets and ligaments and starts rapid vaporization. This rapid evaporation of liquid droplets and ligaments, and its mixing with the surrounding gases, further reduces the density of centerline fluid to cause an exponential increase in the centerline intensity. For the present experiments, the potential core length is defined as the point at which the centerline intensity has the largest axial gradient. The axial gradients were analyzed using the image processing techniques. This point was found to be close to an intensity of 1.0–2.0 for all the cases. A comparison of the centerline intensities for some of the selected cases are shown in Fig. 5b. This figure suggests that

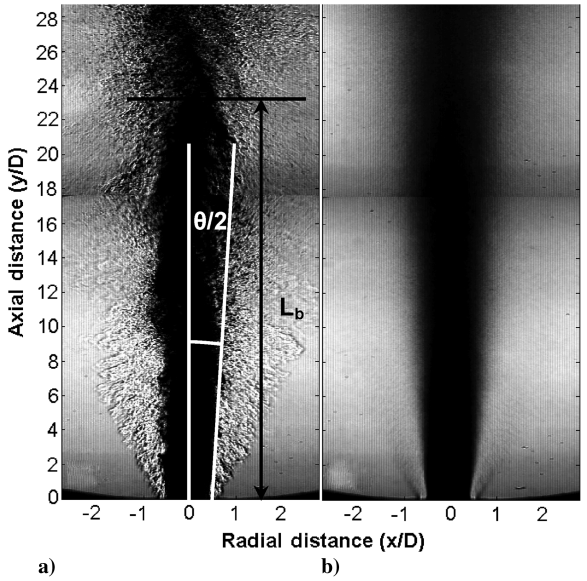

Fig. 2 High-speed schlieren image of LN_2/He flow: a) instantaneous image, b) average of 150 images.

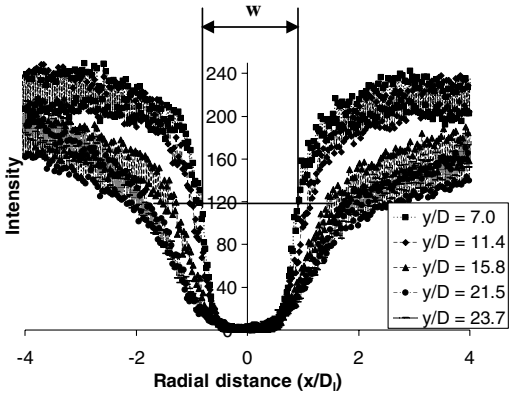

Fig. 3 Radial intensity distribution of LN_2/He flow at various axial locations.

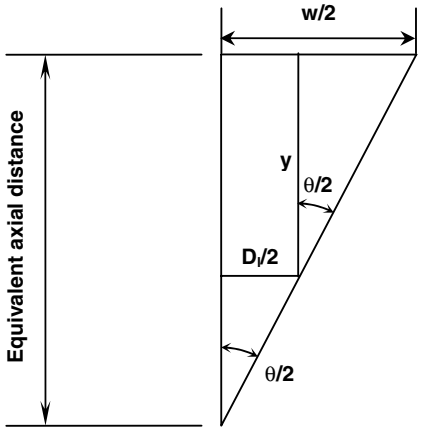

Fig. 4 Description of the parameters used in the calculation of the shear angle of the flow.

gas velocity significantly affects the centerline intensity distribution and, subsequently, the potential core length of the cryogenic fluid jet.

The biggest challenge associated with any quantitative measurement performed at cryogenic flows is uncertainties in the flow behavior. Cryogenic flow itself is a highly unsteady phenomenon due to turbulent behavior and strong heat transfer from the surroundings. These unsteady behaviors are further aggravated by feed pressure fluctuations in line, along with chugging instabilities. Therefore, some kind of error analysis is very crucial for performing any type of quantitative measurements with cryogenic fluids. Most of the previous works lack error analysis of their measurements. We have performed a simple error analysis of potential core length and shear angle measurements to give readers confidence in our data.

Figure 6a shows averaged centerline intensity distribution of LN_2/He flow at 5 m/s and 300 m/s, respectively, repeated over five different times. As one can see, the centerline intensity distributions look completely different for all the cases even though the experimental conditions were kept constant. Table 2 shows the variation in potential core length measurements for the five cases. The percentage variation $(0.5[\max - \min]/\text{mean})$ in the potential core length measurement came out to be approximately $\pm 4.6\%$. This process was repeated for all experimental cases and the maximum variation was found to be approximately $\pm 5.0\%$. The actual potential core length was assumed to be the largest value among the five different cases to get the most conservative estimate, and the values were plotted with error bars showing $\pm 5.0\%$ errors.

Similarly, Fig. 6b shows the variation of light intensity with radial distance for LN_2/He flow at 5 m/s and 300 m/s, respectively, at an axial location of $7D$, repeated over five different times. One can see that all of the five plots almost fell on each other, suggesting very little variation in shear angles. Indeed, the shear angle measurements (Table 2) show no significant variation. The mean for the five cases came out be approximately 5.44, whereas the percentage variation in shear angle was approximately $\pm 5.0\%$ for all the cases. This is due to the fact that shear angles are extremely small, so that even a very minute change in flow width can cause significant variation in the shear angle.

IV. Results and Discussion

In the results, we examine and analyze the effects of changing the velocity of the gaseous stream on the evolutionary behavior of the LN_2 jet upon its exit from the coaxial injector. One important parameter that is used to describe the macrostructure of a jet is shear

Table 2 Variation of LN_2 jet for the same experimental conditions

	Case 1	Case 2	Case 3	Case 4	Case 5
Potential core length	19.0	17.7	19.5	17.5	18.7
Shear angle	5.12	5.66	5.48	5.3	5.66

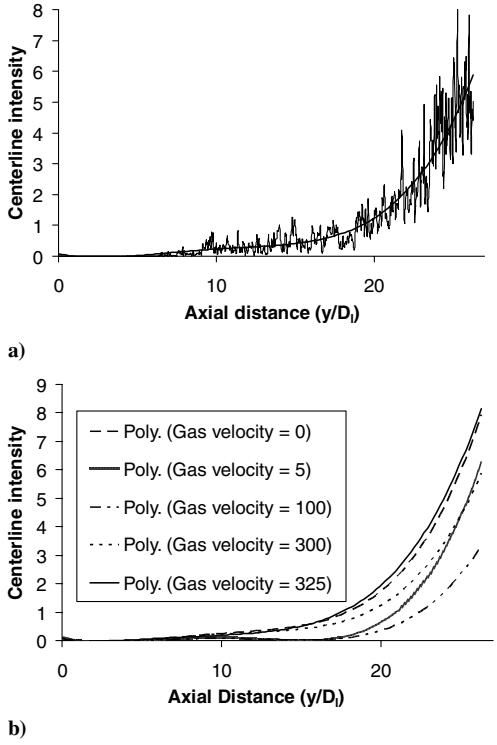

Fig. 5 Averaged centerline intensity distribution of a) LN_2/He flow, b) LN_2/He flow for different velocities of the coaxial gaseous jet.

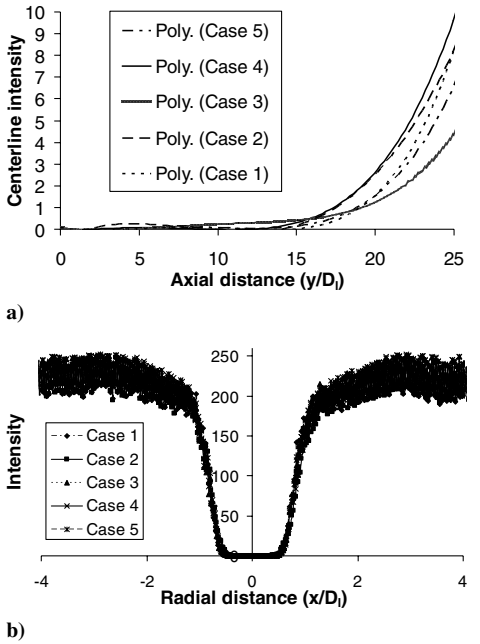

Fig. 6 Averaged intensity variation of LN_2/He flow for the same experimental conditions: a) centerline, b) radial.

or spreading angle. The shear or spreading angle is a direct quantification of the growth rate of shear layer between the fluids, which is directly responsible for the destabilization of the jets. Shear angles for the present set of experiments were measured as discussed in the data analysis section. Figure 7 shows the shear angle of the steady LN_2 jet in quiescent air at different axial locations. The plotted values are the mean for five different experiments at the same location, with the same inlet conditions, with a maximum variation of $\pm 5.0\%$. The definition of the flow width for the present set of experiments was assumed at light intensity of 120 ($I = 120$) as discussed previously. The results for some other values of intensities

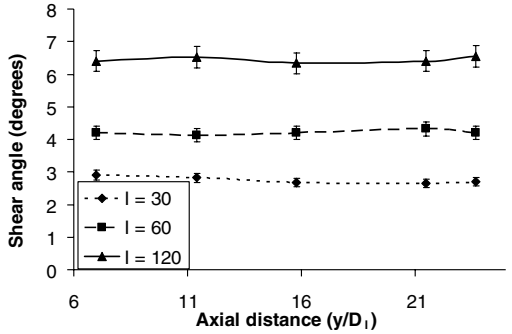

Fig. 7 Shear angle of LN_2 jet in quiescent air at various axial locations.

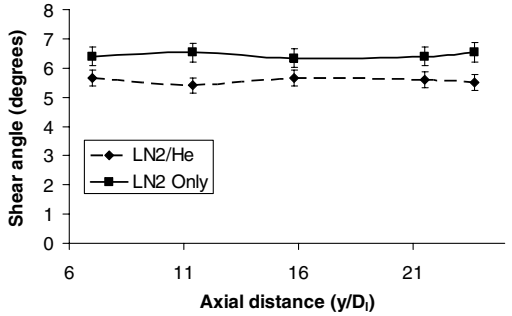

Fig. 8 Shear angles of LN_2 jet in quiescent air and with coaxial helium stream at various axial locations.

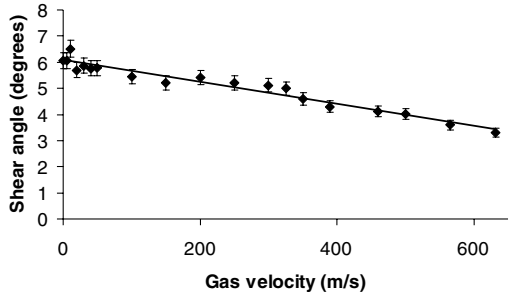

Fig. 9 Shear angle of LN_2/He flow for different velocities of the coaxial helium jet.

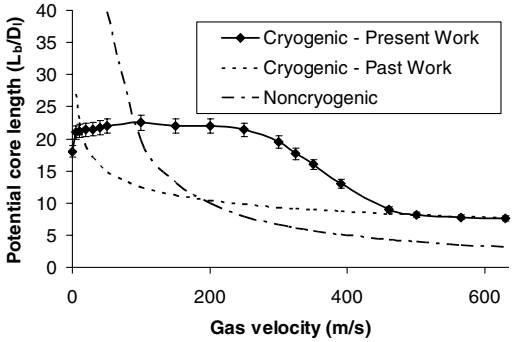

Fig. 10 Potential core length of LN_2 jet for different velocities of the coaxial gaseous jet.

($I = 60$ and 30) were also presented for comparison purposes. As expected, the shear angle of the flow reduced with a decrease in the assumed value of jet width, and it remained relatively constant over the axial distance, thus confirming that the jet is steady and fully developed. The mean shear angle averaged over the axial distance was found to be 6.4, 4.2, and 2.7 deg ±5.0% for $I = 120$, 60, and 30, respectively. The predicted spreading angle for a water jet in quiescent air was approximately 0.6 deg using Reitz and Bracco's correlation [8] [$\theta \approx 0.27(\rho_g/\rho_l)^{0.5}$], whereas it was approximately 1.2 and 8.4 deg for subcritical and supercritical LN_2 jets, respectively, using Chehroudi et al.'s correlation [9,10] $\theta = 0.27\{F[x(\rho_g/\rho_l)] + (\rho_g/\rho_l)^{0.5}\}$. The measured value for our experiment was in between the predicted values for subcritical and supercritical cases. This was due to the fact that the LN_2 jet in our case is injected into the atmosphere at subcritical pressure (1 atm) and supercritical temperature (295 K). Also, the cooling effect of the LN_2 jet on surrounding air increased the density of the surrounding air, and thus increased the shear or spreading angle.

To further investigate these effects, the shear angles were measured for the LN_2 jet in a coaxial helium stream at 300 m/s (LN_2/He) (see Fig. 8). As one can see, the shear angles for both of the flows are constant over the axial distance, however, the shear angle of the LN_2/He flow is smaller than the shear angles of the LN_2 jet in quiescent air. This further confirmed the effect of surrounding gas density on liquid-jet spreading. The flow of helium reduced the effective density of the surrounding air, thus reducing the jet spread. However, even for the helium case, the shear angle was higher than the predicted value, which shows the effect of heat transfer and transcritical behavior, along with the entrainment of surrounding air into the coaxial gaseous flow.

Figure 9 shows the shear angles of all the cases averaged over axial distance and plotted against the coaxial helium velocity. The predicted spreading angles for the LN_2 jet in quiescent helium were approximately 0.7 and 8.0 deg for subcritical and supercritical pressures using Chehroudi et al.'s correlation [9,10]. It can be seen that the shear angle decreased uniformly with increase in coaxial helium velocity and moved toward the predicted value. This further proved our assertion that injection of helium reduced the density of the surrounding medium, thus reducing the jet spread. As the velocity of the helium jet increased, the mass flow rate of helium gas injected into the surrounding air increased, thus reducing the effective density of the surrounding medium.

Another important parameter that is used to describe the macrostructure of a jet is the potential core length. The potential core lengths for the various cases calculated, as discussed in the data analysis section, are shown in Table 2 (note that LN_2 Reynolds and Weber numbers were kept constant at 2.21E + 05 and 1.93E + 04, respectively). Figure 10 shows the potential core length of LN_2 with coaxial helium velocity. The predicted potential core lengths, as proposed by previous researchers [4,24], have also been plotted for the purposes of comparison. As one can see, present results do not match at all with the predicted potential core length of the noncryogenic jet (water), however, they match really well with the predicted core length of the cryogenic jet at higher gas velocities or momentum ratio between the jets. This is due to the fact that the correlation used for the cryogenic jet was experimentally validated for only higher values of momentum ratios ($M \geq 2$). This further supports the uniqueness of our results because it matched extremely well with the results obtained by a different laboratory under a similar set of conditions.

A close examination of Fig. 10 reveals some interesting features. The potential core length of the LN_2 jet increases with the increase in velocity of the gaseous jet, until this velocity reaches a value of about 100 m/s, beyond which the potential core length of the liquid jet drops. In contrast to these results, previous research had suggested that the potential core length of the liquid jet should decrease absolutely with the increase in velocity of the gaseous jet, because this increases the momentum ratio between the jets. These suggestions are undoubtedly accurate, if the liquid jet is a subcritical isothermal fluid (water, for example). The unique behavior of the LN_2 jet is, however, due to the heat transfer effects of the surroundings on the supercritical LN_2 jet. Most of the previous research, conducted on the characterization of the potential core length of a liquid jet inside a coaxial gaseous one, has either been on noncryogenic fluids, where the heat transfer effects were negligible, or on cryogenic fluids but at very high gas velocities compared to the liquid velocity. However, the case is substantially different for a cryogenic LN_2 jet that is being injected in warm surroundings with a gas velocity comparable to the LN_2 velocity.

The vaporization of LN_2 due to the heat transfer from the surroundings has an effect as significant as that of the shearing of the surrounding gaseous jet on the breakup of the LN_2 jet. In light of this vitally important fact, the discrepancy observed in Fig. 10 between the results of this work and those of previous research can be explained as follows. Initially, when LN_2 is injected solely, with no coaxial gaseous jet, the LN_2 jet is in direct contact with the atmosphere (295 K), which acts as a heat source for the cold jet (77 K). The heat transfer from the surrounding atmosphere makes the central core vaporize faster and break sooner, resulting in a shorter potential core length than the noncryogenic jet. Another important feature of Fig. 10 is a longer potential core length of the cryogenic LN_2 jet than noncryogenic ones at higher gas velocities. This is due to another effect of heat transfer from the coaxial gaseous jet to the cold LN_2 jet. The moment the coaxial gaseous jet comes in contact with the cold LN_2 jet, an infinitesimally small layer of gaseous nitrogen forms at the interface of the two fluids. This gaseous nitrogen layer expands radially outward and pushes the coaxial gas away from the LN_2 jet, which in turn reduces the shearing effect of the coaxial gaseous jet on the central cryogenic jet. This reduction in the shearing effect causes the larger liquid core lengths at higher helium jet velocities.

The introduction of coaxial gas has two major effects on the cryogenic jet, that is, shear-layer destabilization and heat transfer. The effect of heat transfer is controlled by the gaseous jet Reynolds number Re_g and the Prandtl number ($Pr_g = \mu Cp/k$). For a constant Prandtl number Pr_g, when the gaseous jet is at lower velocity, it acts like a heat shield for the cold cryogenic jet, whereas this effect does not remain prominent at higher velocities of the coaxial gas. This phenomenon can be explained by taking a look at the gas Reynolds number on potential core length of the cryogenic jet (Fig. 11). At lower velocities, the gaseous jet is laminar, and so convective heat transfer is minimal, but heat conduction from the surroundings is reduced because the gaseous jet creates a thermal insulation around the cold LN_2 jet, due to its really low thermal conductivity. Convective heat transfer increases with an increase in Reynolds number, but conduction decreases as a thicker layer of gas now surrounds the liquid jet and shields it from the surrounding warm atmosphere which acts as a heat source, and so those effects start balancing each other out. As the Reynolds number further increases, the flow reaches a fully developed turbulent condition so that heat transfer is completely controlled by convection and the effect of heat shielding becomes negligible.

The effect of shear-layer destabilization, which has been explained in previous works [4,24,29], is controlled by momentum ratio between the jets (Fig. 12) and is generally negligible for momentum ratios less than one ($M \ll 1$). Shear-layer destabilization starts increasing at momentum ratios close to one ($M \sim 1$) and become significant for momentum ratios greater than one ($M > 1$). Figure 12 also confirms the exponential decay of potential core length with momentum ratio for values close to and higher than one, as predicted by Davis and Chehroudi [29].

At low helium velocities (up to about 100 m/s), the destabilization of LN_2 due to the shearing effects of helium is still minor and not quite effective. However, the destabilization due to heat transfer, which is the dominant mode of destabilization at these conditions, gets affected by the introduction of helium, which results in longer potential cores, as the helium velocity is slightly increased. Close to a helium velocity of 100 m/s, the heat-shielding effect of the helium jet reaches its maximum, whereas the shear-layer effect is still negligible, which makes the potential core length achieve a local maximum. When the helium velocity reaches approximately 300 m/s, the heat-shielding effect of the helium jet starts diminishing due to an increase in convective heat transfer, whereas the shear-layer destabilization effect starts increasing exponentially to cause a steep reduction in potential core length. At a helium velocity of about 325 m/s ($M \approx 1$), the potential core length of the LN_2 jet becomes even shorter than the corresponding case without the helium jet, which suggests that, at 325 m/s and beyond, the effect of shear-layer destabilization of helium on the LN_2 jet has finally prevailed over the helium heat-shielding effect completely.

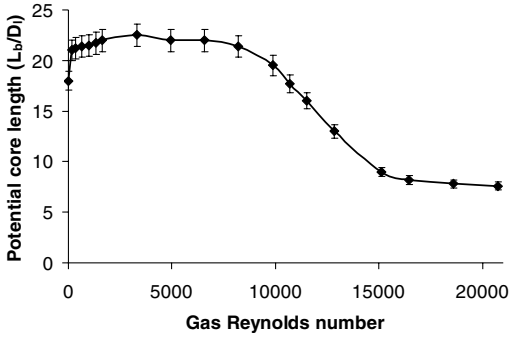

Fig. 11 Variation of potential core length of LN_2 jet Reynolds number of the gaseous jet.

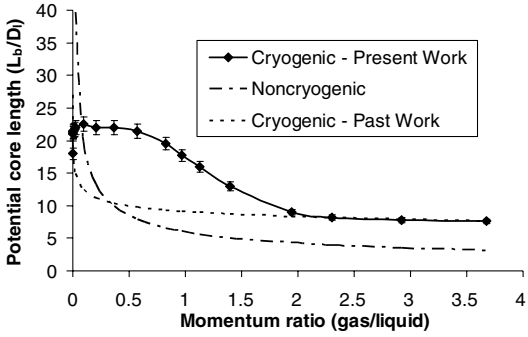

Fig. 12 Variation of potential core length of LN_2 jet with momentum ratio between the jets.

V. Conclusions

The effects of some of the most important flow parameters, such as the velocity, density, and momentum ratios of a flow emerging from a single-element coaxial rocket engine injector, have been examined experimentally over a range of experimental conditions that encompass many of the practical injector operating conditions in rocket engines. The flow conditions examined are characteristic of the rocket engine conditions at liftoff before ignition to provide a simple analogy and simulation of the flow and mixing behaviors from single-element injectors under relevant rocket engine operating conditions. The potential core length of the cryogenic liquid jet as well as the shear angle of the flow have been examined experimentally, using surrounding gases of different densities and emerging at different velocities.

The shear angle of the flow remained constant along the axial distance, thus confirming fully developed steady-state jet. The mean value showed the transcritical nature of the liquid nitrogen jet under atmospheric conditions. The shear angle of the flow also reduced with introduction of a helium jet and decreased uniformly with an increase in helium jet velocity, which proved the effect of surrounding gas density on the jet spreading as predicted by previous researchers.

The results revealed a key effect of heat transfer from the surroundings on the flow behavior of such an injector flow, which involves a central cryogenic fluid jet surrounded by an outer gaseous one. The effect of momentum ratio was found to be pronounced as well, but only for values close to and greater than one. The potential core length of the cryogenic LN_2 showed a local peak when plotted versus the velocity of the gaseous jet. In contrast to the present results, previous research has suggested that the potential core length of the liquid jet should decrease absolutely with the increase in velocity of the gaseous jet, because this increases the momentum ratio between the jets. These suggestions are undoubtedly accurate, if the liquid jet is a subcritical isothermal fluid (e.g., water). The unique behavior of the LN_2 jet is, however, due to the heat transfer effects of the surroundings on the LN_2 jet. The results provide strong evidence

of the heat-shielding effect of the coaxial gaseous jet. The heat transfer from the surroundings to the cold LN_2 jet is reduced significantly by the presence of the gaseous jet, which strongly affects the potential core length of the LN_2 jet.

A combination of the nonintrusive schlieren diagnostic technique and digital image processing has allowed us to examine the detailed features of the cryogenic injector jet under simulated rocket engine operating conditions. The results of this work provide insightful information on the flow and mixing behaviors of a cryogenic jet inside a coaxial gaseous stream. Moreover, these results can also be used to validate computational models under nonreacting flow conditions.

Acknowledgments

This work was supported by the Space Vehicle Technology Institute under grant NCC3-989, jointly funded by NASA and the U.S. Department of Defense within the NASA Constellation University Institutes Project, with Claudia Meyer as the Project Manager. Technical support provided by Kenneth H. Yu, Martin B. Linck, and Ahmed Abdelhafez is greatly appreciated.

References

[1] Sutton, G. P., and Biblarz, O., *Rocket Propulsion Elements*, 7th ed., Wiley, New York, 2001, Chaps. 6–8.

[2] Raynal, L., "Instabilite et Entrainement à l'interface d'une Couche de Melange Liquide-Gaz," Ph.D. Thesis, Université Joseph Fourier, Grenoble, France, 1997.

[3] Bellan, J., "Supercritical (and Subcritical) Fluid Behavior and Modeling: Drops, Streams, Shear and Mixing Layers, Jets and Sprays," *Progress in Energy and Combustion Science*, Vol. 26, Nos. 4–6, 2000, pp. 329–366. doi:10.1016/S0360-1285(00)00008-3

[4] Lasheras, J. C., and Hopfinger, E. J., "Liquid Jet Instability and Atomization in a Coaxial Gas Stream," *Annual Review of Fluid Mechanics*, Vol. 32, Jan. 2000, pp. 275–308. doi:10.1146/annurev.fluid.32.1.275

[5] Huzel, D., and Huang, D., *Modern Engineering for Design of Liquid Propellant Rocket Engines*, Vol. 147, Progress in Astronautics and Aeronautics, AIAA, Washington, D.C., 1992, pp. 104–110.

[6] Vingert, L., Gicquel, P., Lourme, D., and Menoret, L., "Coaxial Injector Atomization," *Liquid Rocket Engine Combustion Instability*, edited by V. Yang, and W. E. Anderson, Vol. 169, Progress in Astronautics and Aeronautics, AIAA, Washington, D.C., 1994, pp. 145–189.

[7] Mayer, W., and Smith, J. J., "Fundamentals of Supercritical Mixing and Combustion of Cryogenic Propellants," *Liquid Rocket Thrust Chambers: Aspects of Modeling, Analysis and Design*, edited by V. Yang, M. Habiballah, M. Popp, and J. Hulka, Vol. 200, Progress in Astronautics and Aeronautics, AIAA, Washington, D.C., 2004, pp. 339–367.

[8] Reitz, R. D., and Bracco, F. V., "Mechanisms of Atomization of a Liquid Jet," *Physics of Fluids*, Vol. 25, No. 10, Oct. 1982, pp. 1730–1742. doi:10.1063/1.863650

[9] Chehroudi, B., Cohn, R., and Talley, D. G., "Cryogenic Shear Layers: Experiments and Initial Growth Rates of Round Cryogenic Jets at Subcritical and Supercritical Pressures," *International Journal of Heat and Fluid Flow*, Vol. 23, No. 5, 2002, pp. 554–563. doi:10.1016/S0142-727X(02)00151-0

[10] Chehroudi, B., Talley, D. G., and Coy, E. B., "Visual Characteristics and Initial Growth Rates of Round Cryogenic Jets at Subcritical and Supercritical Pressures," *Physics of Fluids*, Vol. 14, No. 2, Feb. 2002, pp. 850–861. doi:10.1063/1.1430735

[11] Gautam, V., and Gupta, A. K., "Simulation of Mixing in Rocket Engine Injector Under In-Space Conditions," *41st AIAA/ASME/ASME/SAE/ASEE Joint Propulsion Conference*, AIAA Paper 2005-1445, July 2005.

[12] Strakey, P. A., Talley, D. G., and Hutt, J. J., "Mixing Characteristics of Coaxial Injectors at High Gas/Liquid Momentum Ratios," *Journal of Propulsion and Power*, Vol. 17, No. 2, March–April 2001, pp. 402–410.

[13] Villermaux, E., "Mixing and Spray Formation in Coaxial Jets," *Journal of Propulsion and Power*, Vol. 14, No. 5, Sept.–Oct. 1998, pp. 807–817.

[14] Villermaux, E., and Rehab, H., "Mixing in Coaxial Jets," *Journal of Fluid Mechanics*, Vol. 425, No. 1, Dec. 2000, pp. 161–185. doi:10.1017/S002211200000210X

[15] Farago, Z., and Chigier, N., "Morphological Classification of Disintegration of Round Liquid Jets," *Atomization and Sprays*, Vol. 2, No. 2, 1992, pp. 137–153.

[16] Rehab, H., Villermaux, E., and Hopfinger, E. J., "Flow Regimes of Large Velocity Ratio Coaxial Jets," *Journal of Fluid Mechanics*, Vol. 345, No. 1, Aug. 1997, pp. 357–381. doi:10.1017/S002211209700637X

[17] Lasheras, J. C., Villermaux, E., and Hopfinger, E. J., "Breakup and Atomization of a Round Jet by a High Speed Annular Air Jet," *Journal of Fluid Mechanics*, Vol. 357, No. 1, Feb. 1998, pp. 351–379. doi:10.1017/S0022112097008070

[18] Pal, S., Moser, M. D., Ryan, H. M., Foust, M. J., and Santero, R. J., "Shear Coaxial Injector Atomization Phenomena for Combusting and Non-Combusting Conditions," *Atomization and Sprays*, Vol. 6, No. 2, 1996, pp. 227–244.

[19] Vingert, L., Gicquel, P., Ledoux, M., Care, I., Micci, M., and Glogowski, M., "Atomization in Coaxial Jet Injectors," *Liquid Rocket Thrust Chambers: Aspects of Modeling, Analysis and Design*, edited by V. Yang, M. Habiballah, M. Popp, and J. Hulka, Vol. 200, Progress in Astronautics and Aeronautics, AIAA, Reston, VA, 2004, pp. 105–140.

[20] Mayer, W., and Tamura, H., "Propellant Injection in a Liquid Oxygen/Gaseous Hydrogen Rocket Engine," *Journal of Propulsion and Power*, Vol. 12, No. 6, Nov.–Dec. 1996, pp. 1137–1147. doi:10.2514/3.24154

[21] Mayer, W., Schik, A., Vielle, B., Chauveau, C., Gokalp, I., Talley, D., and Woodward, R., "Atomization and Breakup of Cryogenic Propellants Under High Pressure Subcritical and Supercritical Conditions," *Journal of Propulsion and Power*, Vol. 14, No. 5, Sept.–Oct. 1998, pp. 835–842.

[22] Mayer, W., Schik, A., Schaffler, M., and Tamura, H., "Injection and Mixing Processes in High Pressure Liquid Oxygen/Gaseous Hydrogen Rocket Combustors," *Journal of Propulsion and Power*, Vol. 16, No. 5, Sept.–Oct. 2000, pp. 823–828.

[23] Mayer, W., Ivancic, B., Schik, A., and Hornung, U., "Propellant Atomization and Ignition Phenomena in Liquid Oxygen/Gaseous Hydrogen Rocket Combustors," *Journal of Propulsion and Power*, Vol. 17, No. 4, July–Aug. 2001, pp. 794–799.

[24] Porcheron, E., Carreau, J. L., Prevost, L., Le Visage, D., and Roger, F., "Effect of Injection Gas Density on Coaxial Liquid Jet Atomization," *Atomization and Sprays*, Vol. 12, No. 1, 2002, pp. 209–227. doi:10.1615/AtomizSpr.v12.i123.110

[25] Oschwald, M., Smith, J. J., Branam, R., Hussong, J., Schik, A., Chehroudi, B., and Talley, D., "Injection of Fluids into Supercritical Environments," *Combustion Science and Technology*, Vol. 178, Nos. 1–3, 2006, pp. 49–100. doi:10.1080/00102200500292464

[26] Gautam, V., and Gupta, A. K., "Simulation of Flow and Mixing from a Coaxial Rocket Injector," *44th AIAA Aerospace Sciences Meeting*, AIAA Paper 2006-1160, Jan. 2006.

[27] Gautam, V., and Gupta, A. K., "Cryogenic Flow and Mixing from a Single Element Coaxial Rocket Injector," *42nd AIAA/ASME/SAE/ASEE Joint Propulsion Conference*, AIAA Paper 2006-4529, July 2006.

[28] Gautam, V., and Gupta, A. K., "Simulation of Flow and Mixing from a Cryogenic Rocket Injector," *Journal of Propulsion and Power*, Vol. 23, No. 1, 2007, pp. 123–130. doi:10.2514/1.19731

[29] Davis, D. W., and Chehroudi, B., "Measurements in an Acoustically Driven Coaxial Jet Under Sub-, Near- and Super-Critical Conditions," *Journal of Propulsion and Power*, Vol. 23, No. 2, March–April 2007, pp. 364–374. doi:10.2514/1.19340

C. Avedisian
Associate Editor